INTERNATIONAL JOURNAL FOR NUMERICAL METHODS IN FLUIDS, VOL. 13, 83–107 (1991)

MULTIPLE-PLANE-JET TURBULENT MIXING ANALYSIS VIA A KINETIC THEORY APPROACH

SHU-HAO CHUANG

Department of Mechanical Engineering, National Chung-Hsing University, Taichung, Taiwan 40227, R.O.C.

ZUU-CHANG HONG

Department of Mechanical Engineering, National Central University, Chungli, Taiwan 32054, R.O.C.

AND

JHY-HORNG WANG

Department of Power Mechanical Engineering, National Tsing-Hua University, Hsinchu, Taiwan 30043, R.O.C.

SUMMARY

Turbulent mixing of a single jet, twin jets, triple jets and multiple jets is synthetically analysed in this paper. Chung's kinetic theory of turbulence and a modified Green's function are employed to solve this problem. The probability density function of fluid elements in the velocity space of multiple plane jets and the corresponding turbulence correlations are revealed in this analysis. The calculated results are found to be in good agreement with the available experimental data. The internal physical structure of the turbulent mixing mechanism seems better understood via the kinetic theory approach. The present study provides the fundamentals for theoretical understanding of multiple-jet turbulent mixing and further application to multiple-jet turbulent combustion analysis.

KEY WORDS Kinetic theory of turbulence Multiple jets Turbulent mixing PDF

INTRODUCTION

In some gas burners the gas stream is subdivided into a number of single jets. The gas stream emerges from the various parallel jets. Depending on the distance between the single openings, more or less interaction between jets takes place. The mutual interaction of multiple-jet flow is very complicated. The flame length and flame width of gas burners are affected by the mutual interaction of multiple jets. Therefore study of the multiple-jet turbulent mixing problem is very important from a practical viewpoint. Analysis of a single plane jet via kinetic theory is the basic observation of multiple jets through a statistical approach.[1] Studies of twin plane jets[2] provide some basic understanding of the mutual interaction of multiple jets. The objectives of Reference 2 were limited to studies of twin-jet flow fields; the mutual interaction of multiple jets ($n \geqslant 3$) was not considered. The present paper is mainly concerned with the five-parallel-jet turbulent mixing problem via a kinetic theory approach. In order to complete the synthetic analysis of multiple jets, some results of single- and twin-jet flow are deduced from References 1, 2 and 39.

Several approaches to turbulence modelling descriptions have been proposed in recent years. Most of them have been developed from the concept of gradient-type transport. The present work

0271–2091/91/110083–25$12.50

Received October 1989
Revised July 1990

is an alternative approach to turbulence modelling which seeks a probability density function (PDF) to characterize the stochastic characteristics of fluid elements in the velocity space. It is a kinetic theory approach. Since 1967 there have been a number of turbulent kinetic theories proposed.[3-10] A Langevin model appropriate to constant-property turbulent flows was developed from the general equation for the fluid particle velocity increment proposed by Pope.[11] The objective of Pope's work was to determine the form of a second-order tensor appearing in the general model equation as a function of local mean quantities. A modelled transport equation for the joint probability density function (JPDF) of the velocities and a scalar has been solved numerically for four self-similar turbulent free shear flows.[8] In this context, modifications to the Langevin equation have been made both to the deterministic term and to the form of the random term.[12,13] These theories were limited to studies of flow without chemical reaction. A more general kinetic theory of turbulence for chemically reacting flows was developed by Chung.[14-21] Chung's equation was solved by Hong[22] using Green's function to directly integrate the equation for the PDF. This method was successfully modified for free shear layer mixing and combustion problems.[1,23] In the modified Green's function method the authors actually solved an instantaneous mixing problem to simulate the steady state phenomenon. These previous studies[1,23] demonstrated the inherent advantages of the Green's function method for solving Chung's kinetic turbulence equations. Thus the present investigations of multiple plane jets using the Green's function method for construction of the PDF are warranted.

Early experimental work on multiple jets was done by Corrisin,[24] who studied the flow from a seven-parallel-slot nozzle. Laurence and Benninghoff[25] studied the flow emanating from four rectangular lobes. The gross characteristics of the flow field emanating from rectangular lobes in a line was reported by Marsters.[26] The flow emanating from a series of closely spaced holes in a line was studied experimentally by Knystautas.[27] Overall aerodynamic studies were made by Aiken[28] on an ejector with multiple rectangular lobes with various spacing-to-width ratios and nozzle dimensions. All these investigations were limited to measurements of lower-order mean quantities. Krothapalli[29,30] made an experimental study of a rectangular jet in a multiple-jet configuration. In order to study the structure of the multiple jets, he also measured the Reynolds stress. In the present analysis, Krothapalli's experimental data have been used as a comparison for our calculated results.

THEORETICAL MODEL

Kinetic equation and Green's function

The kinetic theory approach utilizes the probability density function (PDF) to describe the turbulent field. The definition of the PDF for a fluctuating turbulent velocity field is analogous to that for molecular velocity. The description of the engineering interest flow is based on the probability density function $f(t, \mathbf{x}, \mathbf{u})$ in the present analysis. From the definition of the PDF, $f\mathbf{du}$ represents the probability of finding a fluid element at time t in location $\mathbf{x}$ with its instantaneous velocities in the range between $\mathbf{u}$ and $\mathbf{u}+\mathbf{du}$. If the fluid element has a concentration of a scalar quantity $c(t, \mathbf{x}, \mathbf{u})$, then the PDF of this scalar is $F(t, \mathbf{x}, \mathbf{u}) = c(t, \mathbf{x}, \mathbf{u}) \times f(t, \mathbf{x}, \mathbf{u})$.[14] The derivation of the governing equation for $F(t, \mathbf{x}, \mathbf{u})$ is analogous to that of the Boltzmann equation in the kinetic theory of gases. The derivation of the governing equation for F as applied to multiple-jet mixing can be found elsewhere.[14,22,31,32] The governing equation for F can be written as

$$\frac{\partial F}{\partial t} + u_j \frac{\partial F}{\partial x_j} = \beta \frac{\partial}{\partial u_j}(u_j - \langle u_j \rangle)F + \frac{\beta_1}{3} E \frac{\partial^2 F}{\partial u_j \partial u_j} + \omega f, \tag{1}$$

where

$$\beta=\beta_1+\beta^v, \qquad F=fc, \qquad F_i=fc_i, \qquad \Sigma F_i=f\Sigma c_i=f.$$

In the present analysis we consider that there is no chemical reaction, so $c=1$ and $\omega=0$. Equation (1) then can be written as

$$\frac{\partial f}{\partial t}+(k_j-\beta u_j)\frac{\partial f}{\partial u_j}+u_j\frac{\partial f}{\partial x_j}=3\beta f+q_1\frac{\partial^2 f}{\partial u_j\partial u_j}, \tag{2}$$

where

$$k_j\equiv\beta\langle u_j\rangle, \qquad q_1\equiv\tfrac{1}{3}\beta_1 E.$$

Hong[22] obtained the Green's function of equation (2) as

$$G(\mathbf{x},\mathbf{u},t/\mathbf{x}_0,\mathbf{u}_0,t_0)=\frac{e^{3\beta t}}{8\pi^3(AC-B^2)^{3/2}}$$

$$\times\exp\left(\left(-C\left|\left(\mathbf{u}-\frac{\mathbf{k}}{\beta}\right)e^{\beta t}-\left(\mathbf{u}_0-\frac{\mathbf{k}}{\beta}\right)e^{\beta t_0}\right|^2\right.\right.$$

$$+2B\left[\left(\mathbf{u}-\frac{\mathbf{k}}{\beta}\right)e^{\beta t}-\left(\mathbf{u}_0-\frac{\mathbf{k}}{\beta}\right)e^{\beta t_0}\right]\cdot\left[(\mathbf{x}-\mathbf{x}_0)+\frac{\mathbf{u}-\mathbf{u}_0}{\beta}-\frac{\mathbf{k}}{\beta}(t-t_0)\right]$$

$$\left.\left.+A\left|(\mathbf{x}-\mathbf{x}_0)+\frac{(\mathbf{u}-\mathbf{u}_0)}{\beta}-\frac{\mathbf{k}}{\beta}(t-t_0)\right|^2\right)\Big/(2(AC-B^2))\right), \tag{3}$$

where

$$A\equiv 2\int_{t_0}^{t}q_1 a(\xi)\mathrm{d}\xi, \qquad B\equiv -2\int_{t_0}^{t}q_1 b(\xi)\mathrm{d}\xi, \qquad C\equiv 2\int_{t_0}^{t}q_1 c(\xi)\mathrm{d}\xi, \tag{4}$$

with

$$a=e^{2\beta t}, \qquad b=\frac{1}{\beta}e^{\beta t}, \qquad c=\frac{1}{\beta^2}.$$

Simulation of the flow field

We consider that five turbulent streams of the same mean velocities and turbulence energies are initially separated by five infinitely long thin films (see Figure 2(a)). At $t=t_0$, these thin films are suddenly removed and the five streams begin to mix, as shown in Figure 2(a). This instantaneous mixing phenomenon will be used to simulate the steady state of the five jet mixing problem.[1,23] Assume that an observer begins to move at $t=t_0$ along the x-axis with velocity $\bar{U}_M$, as shown in Figure 2(b). Then the observer will see velocity profiles and other momentum quantities similar to those appearing in Figure 1 for the steady state of five-jet flow. In this simulation the x-axis in the steady state of the five-jet problem may be considered equivalent to $\bar{U}_M t$ in the instantaneous mixing problem. This simulation will be justified by subsequently comparing the calculated results with the experimental data of Spencer[33] and with Lee and Harsha's[34] data. In order to study the turbulent mixing flow for various multiple jets, the individual jets of the five-jet flow are closed

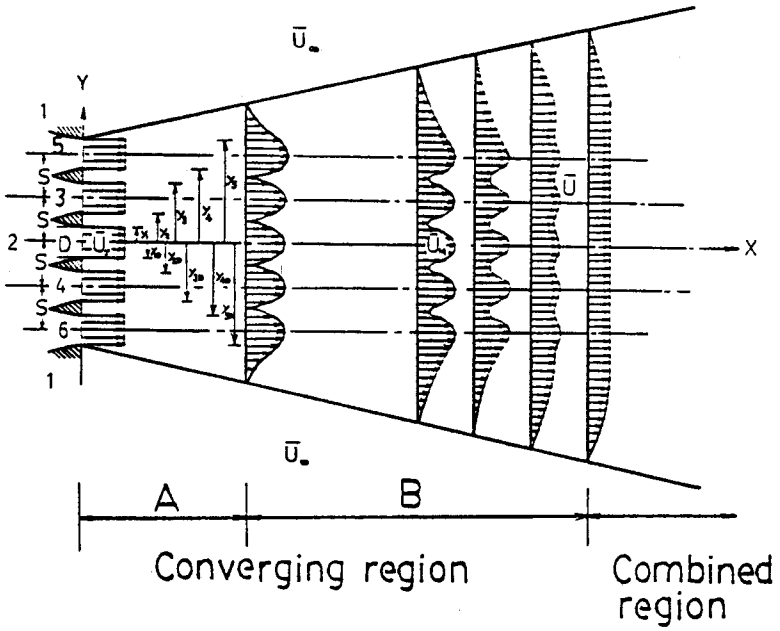

Figure 1. The flow field of multiple plane jets

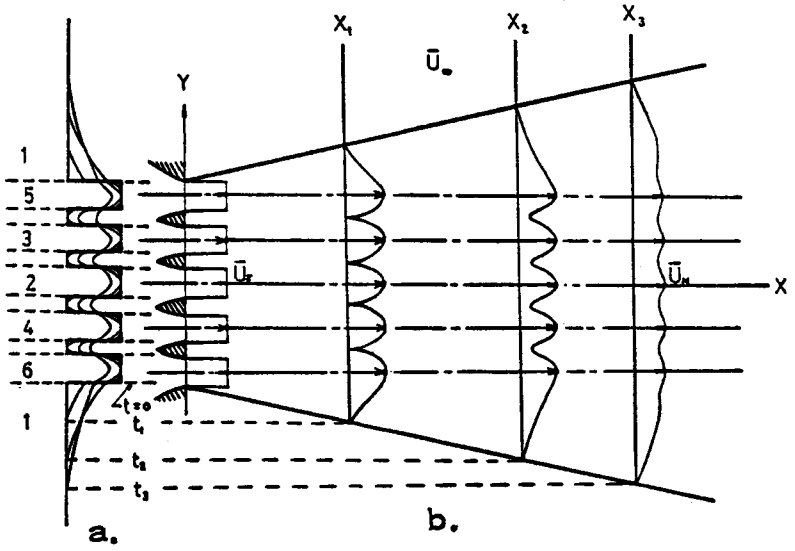

Figure 2. (a) Instantaneous mixing mean velocity profiles observed at fixed X. (b) Mean velocity profiles observed when moving with velocity $\bar{U}_M$

sequentially. The turbulent mixing of a single jet, twin jets, triple jets and multiple jets has been synthetically analysed in this manner.

Source conditions and constructed solution

The obtained Green's function[22] is considered as the instantaneous point source solution of equation (1). In order to utilize this Green's function to construct the PDF, the source conditions

have to be specified according to the given physical problem. Assume that for $t < t_0$ the five streams are homogeneous and their PDFs are Gaussian with respect to their own mean velocities $\bar{U}_j$ and mean turbulent energies E_{0i}. The ambient fluid is also assumed to be homogeneous and its PDF Gaussian with respect to its own mean velocity $\bar{U}_\infty$ and turbulent energy E_{01}. Then the source condition can be written as

$$S_{01} = \frac{1}{(\frac{2}{3}\pi E_{01})^{3/2}} \exp\left(-\frac{(u_0 - \bar{U}_\infty)^2 + v_0^2 + w_0^2}{\frac{2}{3}E_{01}} \right), \tag{5}$$

$$y_1 \leqslant y \leqslant y_2, \qquad y_3 \leqslant y \leqslant y_4, \qquad y_5 \leqslant y,$$
$$y_{2D} \leqslant y \leqslant y_{1D}, \qquad y_{4D} \leqslant y \leqslant y_{3D}, \qquad y \leqslant y_{5D}, \qquad x \leqslant 0,$$

$$S_{0i} = \frac{1}{(\frac{2}{3}\pi E_{0i})^{3/2}} \exp\left(-\frac{(u_0 - \bar{U}_j)^2 + v_0^2 + w_0^2}{\frac{2}{3}E_{0i}} \right), \quad i = 2\text{–}6, \tag{6}$$

$$|y| \leqslant D/2, \qquad y_2 \leqslant y \leqslant y_3, \qquad y_4 \leqslant y \leqslant y_5,$$
$$y_{3D} \leqslant y \leqslant y_{2D}, \qquad y_{5D} \leqslant y \leqslant y_{4D}, \qquad x \leqslant 0,$$

where u_0, v_0, and w_0 are the source's instantaneous velocities in the x-, y- and z-directions respectively. According to the above source conditions, the PDF is constructed as follows:[35]

$$\begin{aligned} f = \int_{-\infty}^{\infty}\int_{-\infty}^{\infty}\int_{-\infty}^{\infty}\int_{-\infty}^{\infty}\int_{-\infty}^{\infty} \Bigg(& \int_{-\infty}^{\infty} GS_{01}\,dy_0 - \int_{y_{5D}}^{y_{4D}} GS_{01}\,dy_0 - \int_{y_{3D}}^{y_{2D}} GS_{01}\,dy_0 \\ & - \int_{y_{1D}}^{y_1} GS_{01}\,dy_0 - \int_{y_2}^{y_3} GS_{01}\,dy_0 - \int_{y_4}^{y_5} GS_{01}\,dy_0 + \int_{y_{5D}}^{y_{4D}} GS_{06}\,dy_0 \\ & + \int_{y_{3D}}^{y_{2D}} GS_{04}\,dy_0 + \int_{y_{1D}}^{y_1} GS_{02}\,dy_0 + \int_{y_2}^{y_3} GS_{03}\,dy_0 + \int_{y_4}^{y_5} GS_{05}\,dy_0 \Bigg) du_0\,dv_0\,dw_0\,dx_0\,dz_0. \end{aligned} \tag{7}$$

The above integration is very tedious.[35] From the constructed PDF, the ensemble average $\langle Q \rangle$ can be obtained as

$$\langle Q \rangle = \int_{-\infty}^{\infty} fQ\,du \tag{8}$$

Let $Q = u_i$, $u_i'^2$, $u_i'u_j'$, $u_i'^2u_j'$; then we can obtain the corresponding relations of first-, second- and third-order turbulence correlations. These integrations are also very tedious.[35] Also, by definition,

$$f(u) = \int_{-\infty}^{\infty}\int_{-\infty}^{\infty} f\,dv\,dw, \qquad f(v) = \int_{-\infty}^{\infty}\int_{-\infty}^{\infty} f\,du\,dw, \tag{9}$$

$$f(u, v) = \int_{-\infty}^{\infty} f\,dw. \tag{10}$$

From the previous analysis and simulation, the X-co-ordinate is expressed as[1]

$$X = \int_0^t \bar{U}_M(t)\,dt = C_2(D/X)\bar{U}_j t. \tag{11}$$

According to the literature,[14,36]

$$\beta_1 = E^{1/2}/2\Lambda, \tag{12}$$

$$\beta^\nu = A'\nu/\lambda^2, \tag{13}$$

where Λ is the characteristic length scale of the turbulence field, λ is the dissipative length scale, ν is the kinematic viscosity and A' is a constant of order unity. By introducing the turbulence Reynolds number

$$Re_\Lambda = E^{1/2}\Lambda/\nu, \tag{14}$$

β^ν can be written in terms of β_1, using equations (13) and (14), as

$$\beta^\nu = b'\beta_1, \tag{15}$$

Table I. The parameter C_1 for different numbers of jets

					$n=1,\ R=0$					
$X/D\backslash\eta$	0·000	0·025	0·050	0·075	0·100	0·125	0·150	0·175	0·200	0·225
5	0·055	0·055	0·048	0·045	0·044	0·037	0·025	0·016	0·010	0·010
30 (over)	0·035	0·036	0·036	0·036	0·033	0·030	0·025	0·019	0·015	0·010
					$n=1,\ R=0{\cdot}16$					
5	0·040	0·042	0·043	0·045	0·042	0·035	0·023	0·015	0·010	0·010
30(over)	0·027	0·028	0·031	0·033	0·032	0·032	0·025	0·017	0·015	0·010
					$n=2,\ \tilde{S}=2,\ R=0$					
$X/D\backslash Y/D$	0·000	0·250	0·500	0·750	1·000	1·250	1·500	1·750	2·000	3·000
5	0·010	0·032	0·050	0·065	0·060	0·054	0·048	0·035	0·020	0·010
20 (over)	0·050	0·052	0·050	0·045	0·040	0·032	0·028	0·020	0·015	0·010
					$n=2,\ \tilde{S}=2,\ R=0{\cdot}3$					
5	0·010	0·028	0·045	0·050	0·045	0·048	0·042	0·030	0·015	0·010
20 (over)	0·040	0·042	0·040	0·038	0·035	0·030	0·028	0·025	0·021	0·010
					$n=2,\ \tilde{S}=11,\ R=0$					
$X/D\backslash Y/D$	0	2	4	6	8	10	12	14		
15	0·010	0·016	0·032	0·040	0·038	0·030	0·020	0·010		
70 (over)	0·038	0·040	0·041	0·038	0·030	0·025	0·015	0·010		
					$n=2,\ \tilde{S}=11,\ R=0{\cdot}3$					
15	0·010	0·012	0·028	0·032	0·028	0·025	0·020	0·010		
70 (over)	0·032	0·035	0·035	0·032	0·025	0·020	0·015	0·010		
					$n=3,\ \tilde{S}=8,\ R=0$					
$X/D\backslash Y/D$	0	1	2	3	4	6	8	10	18	
15	0·088	0·078	0·070	0·055	0·010	0·045	0·078	0·062	0·020	
60 (over)	0·048	0·050	0·050	0·045	0·040	0·038	0·035	0·020	0·010	
					$n=3,\ \tilde{S}=8,\ R=0{\cdot}3$					
15	0·072	0·060	0·055	0·040	0·010	0·032	0·062	0·048	0·015	
60 (over)	0·045	0·048	0·048	0·042	0·036	0·035	0·028	0·020	0·010	
					$n=5,\ \tilde{S}=8,\ R=0$					
$X/D\backslash Y/D$	0	2	4	8	10	14	18	22	26	
15	0·080	0·064	0·010	0·070	0·055	0·015	0·050	0·012	0·010	
80 (over)	0·040	0·042	0·042	0·035	0·025	0·015	0·012	0·010	0·010	
					$n=5,\ \tilde{S}=8,\ R=0{\cdot}3$					
15	0·065	0·050	0·010	0·055	0·040	0·011	0·040	0·010	0·010	
80 (over)	0·038	0·040	0·041	0·032	0·022	0·012	0·010	0·010	0·010	

where

$$b' = 2(\Lambda/\lambda)^2 / Re_\Lambda. \tag{16}$$

According to the previous experimental results,[33, 34] the mixing layer thickness in the flow field is approximately a linear function of X, i.e.

$$\Lambda = C_1' X, \tag{17}$$

where C_1' is a constant. From equations (11), (12) and (17), β_1 can be written as

$$\beta_1 = \frac{E^{1/2}}{C_1 C_2 (D/X) \bar{U}_j t}, \tag{18}$$

where $C_1 = 2C_1'$ and $C_2 = C_2(D/X)$. The constants C_1 and b' are characteristic properties of the turbulence field. Finally, the values of the parameters $b' \approx 0{\cdot}1$ and C_1 are chosen as listed in Table I. Both constants C_1 and b' have been determined; hence equation (8) is described completely.

Processes of calculation

The ensemble averages such as $\langle u_k \rangle$ and $\langle u_k' u_k' \rangle$ appearing in equation (2) are assumed to be known. The equation is linear and the solution of f (PDF) is constructed via linear summation of the weighted Green's functions according to the given source conditions. In order to evaluate $\langle u_k \rangle$ and $\langle u_k' u_k' \rangle$ from equation (8) with $Q = u_k$ and $u_k' u_k'$, one must use an iterative scheme[2] for the correct values of $\langle u_k \rangle$ and $\langle u_k' u_k' \rangle$. All order moments can be constructed from equation (8) when both $\langle u_k \rangle$ and $\langle u_k' u_k' \rangle$ have been determined.

RESULTS AND DISCUSSION

Single jet

In order to compare the results with the available experimental data,[37, 38] two velocity ratios, $R = 0$ and $0{\cdot}16$, are chosen in the present analysis.

Mean velocity. The mean velocity profile in the fully developed region shows very good agreement with Gutmark and Wygnanski's[37] experimental data, as shown in Figure 3. In the present analysis the mean velocity profile $\bar{U}/\bar{U}_0$ has only a small variation (near similarity) with respect to the η-co-ordinate; this result is also seen in Gutmark and Wygnanski's[37] experimental range of X/D from 65 to 118, as shown in Figure 3. The mean velocity profile in the y-direction is shown in Figure 4; the calculated results are lower than the experimental data of Gutmark and Wygnanski.[37] We also find that the mean velocity in the y-direction has little influence on $\bar{U}$, E and the other calculated properties. The mean velocity profiles at a velocity ratio $R = 0{\cdot}16$ are in good agreement with the experimental data of Bradbury,[38] as shown in Figures 5 and 6.

Turbulence energy. The turbulence energy distributions at velocity ratios $R = 0$ and $0{\cdot}16$ are compared with Gutmark and Wygnanski's[37] and Bradbury's[38] experimental data in Figures 7 and 8 respectively. The calculated results in the central region are lower than the experimental data; this may be due to the assumptions made in the present analysis, such as flow without a pressure gradient, etc.

The highest turbulence energy is located in the region $\eta = 0{\cdot}05$–$0{\cdot}1$; this can be interpreted in terms of the development of turbulence energy in the transition region, as shown in Figure 9. As

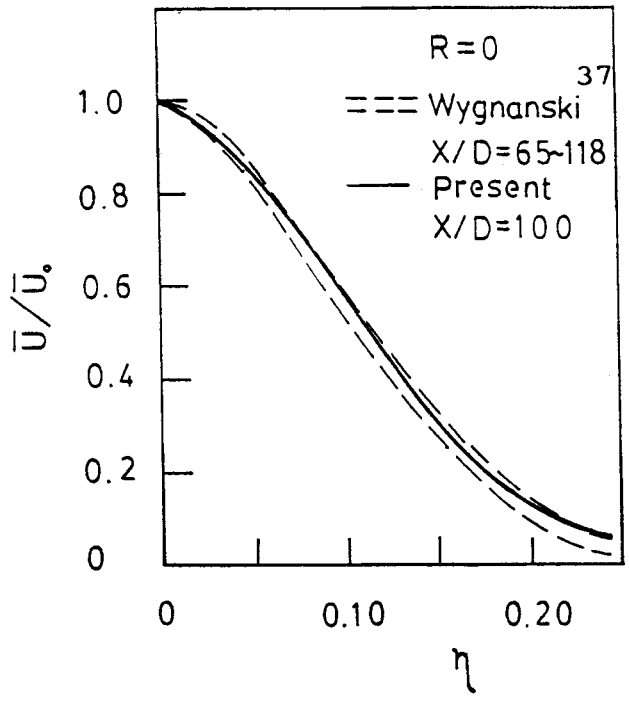

Figure 3. Mean velocity in x-direction ($R=0$)

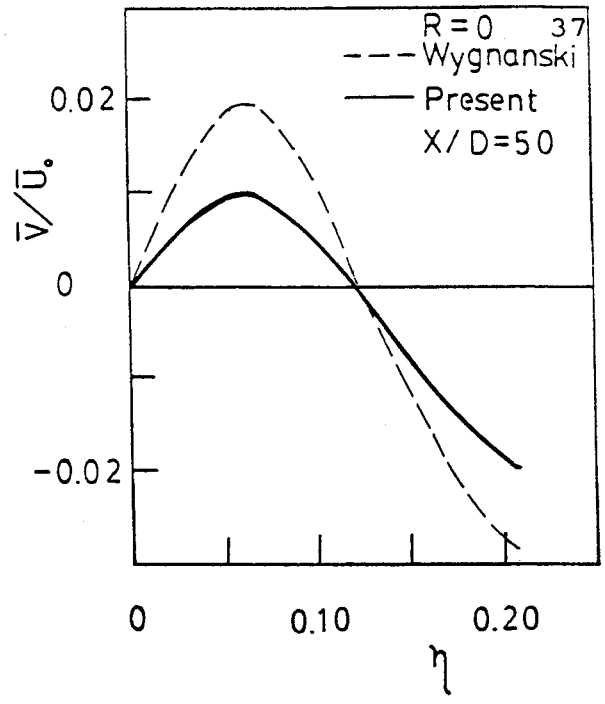

Figure 4. Mean velocity in y-direction ($R=0$)

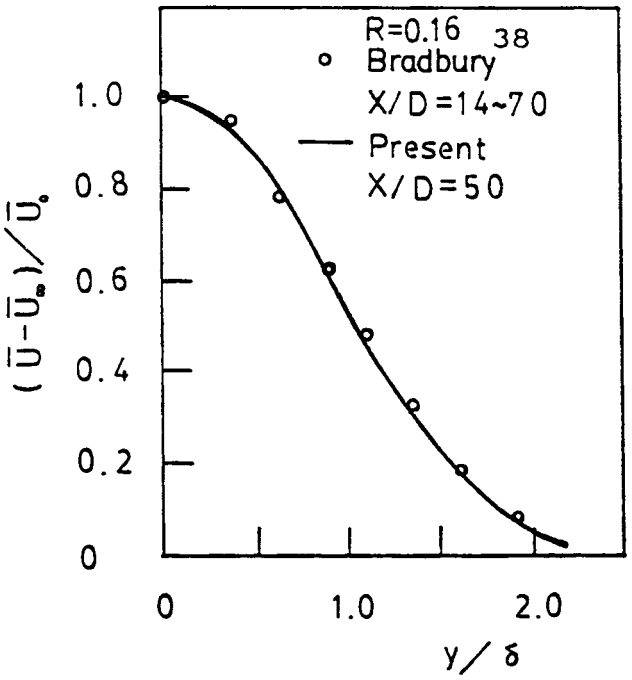

Figure 5. Mean velocity in x-direction ($R=0{\cdot}16$)

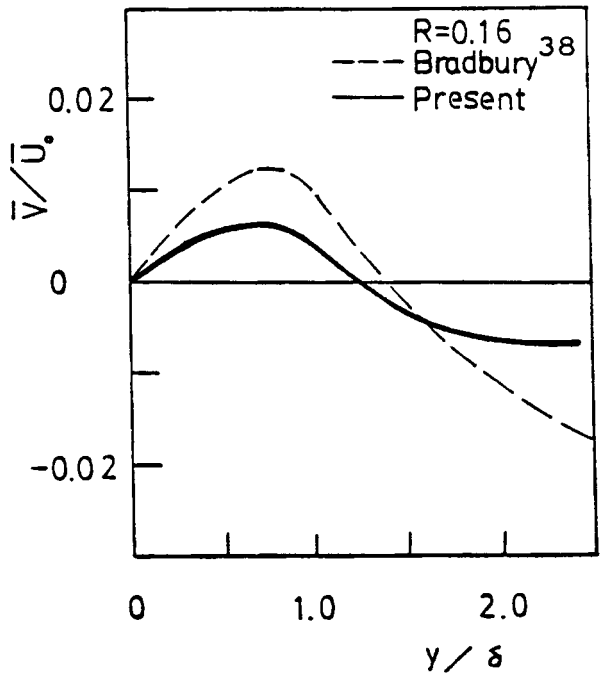

Figure 6. Mean velocity in y-direction ($R=0.16$)

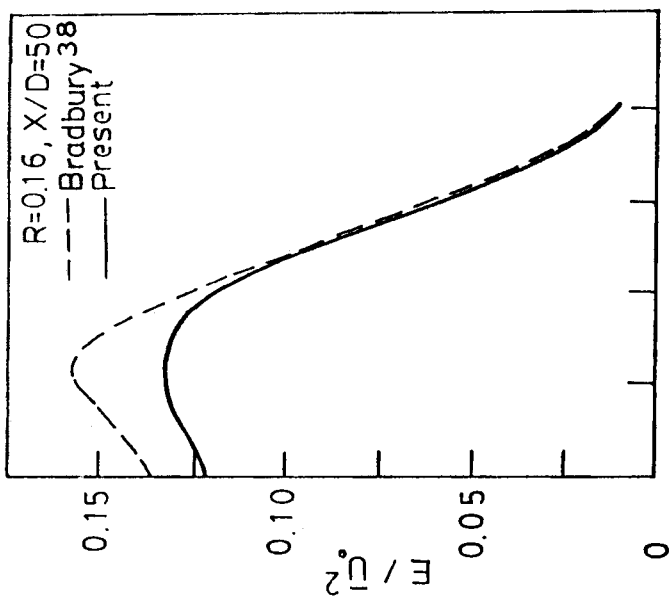

Figure 8. Turbulence energy ($R=0{\cdot}16$)

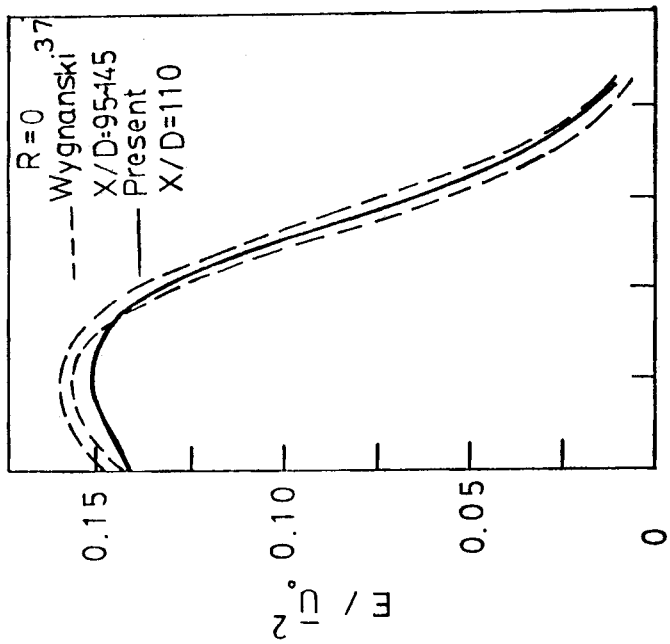

Figure 7. Turbulence energy ($R=0$)

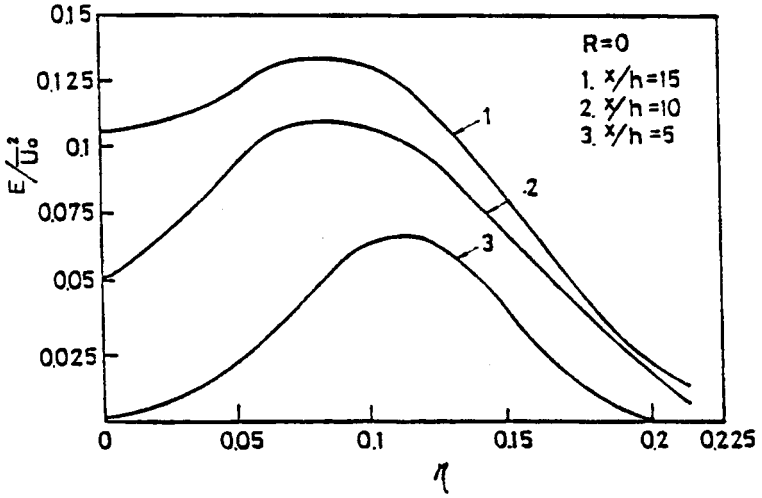

Figure 9. Turbulence energy development in transient region ($R=0$)

mentioned previously, the turbulent jet in the initial region can be considered as two half-jets and the turbulence energy at $\eta=0$ is sharply increased after the potential core disappearance, as shown in Figure 9.

Probability density function (PDF). In the present calculations the standard deviation σ is used as the unit on the horizontal axis. The PDFs of the velocity in the y-direction are shown in Figures 10(a) and 10(b); these functions are close to Gaussian distributions because the velocity in the y-direction is smaller than the velocity in the x-direction. The PDF of u' has two peaks, as shown in Figure 10(c). This phenomenon signifies that the fluid element is influenced by two different eddies from different streams, each still retaining its original characteristic (memory). These characteristics will gradually disappear as it moves towards the outer edge from the centreline, as shown in Figures 10(d) and 10(e). The variation of the joint probability density function (JPDF) along the η-axis indicates turbulent mixing phenomena in the velocity space; two examples are shown in Figures 11(a) and 11(b). At $\eta=0{\cdot}05$ the JPDF deviates from a Gaussian distribution because its corresponding turbulence correlations are strong.

Five jets

In order to utilize the experimental data of Krothapalli,[30] we let the space of the jets be $S=8D$.

Mean velocity. The velocity distributions of the central jet in the x-direction are shown in Figure 12. The calculated results are compared with the experimental data of Krothapalli[30] and show reasonably good agreement. According to Krothapalli's[30] data, mutual interactions among the multiple jets have not occurred for the section $X/D < 15$, so this flow region is a single-jet type. Downstream, the mean velocity in the x-direction gradually becomes flat owing to the mixing between the central jet and the other jets in the region $15 \leqslant X/D \leqslant 60$. In the region $X/D > 60$ the mean velocity is homogeneous owing to the completed turbulent mixing. The mean velocity in the y-direction is shown in Figure 13. From the concept of the continuity equation, we find that the distribution of velocity is reasonable. In the present analysis we also find that the major momentum is in the x-direction; hence the influence of $\bar{V}$ on $\bar{U}$ and E is not important.

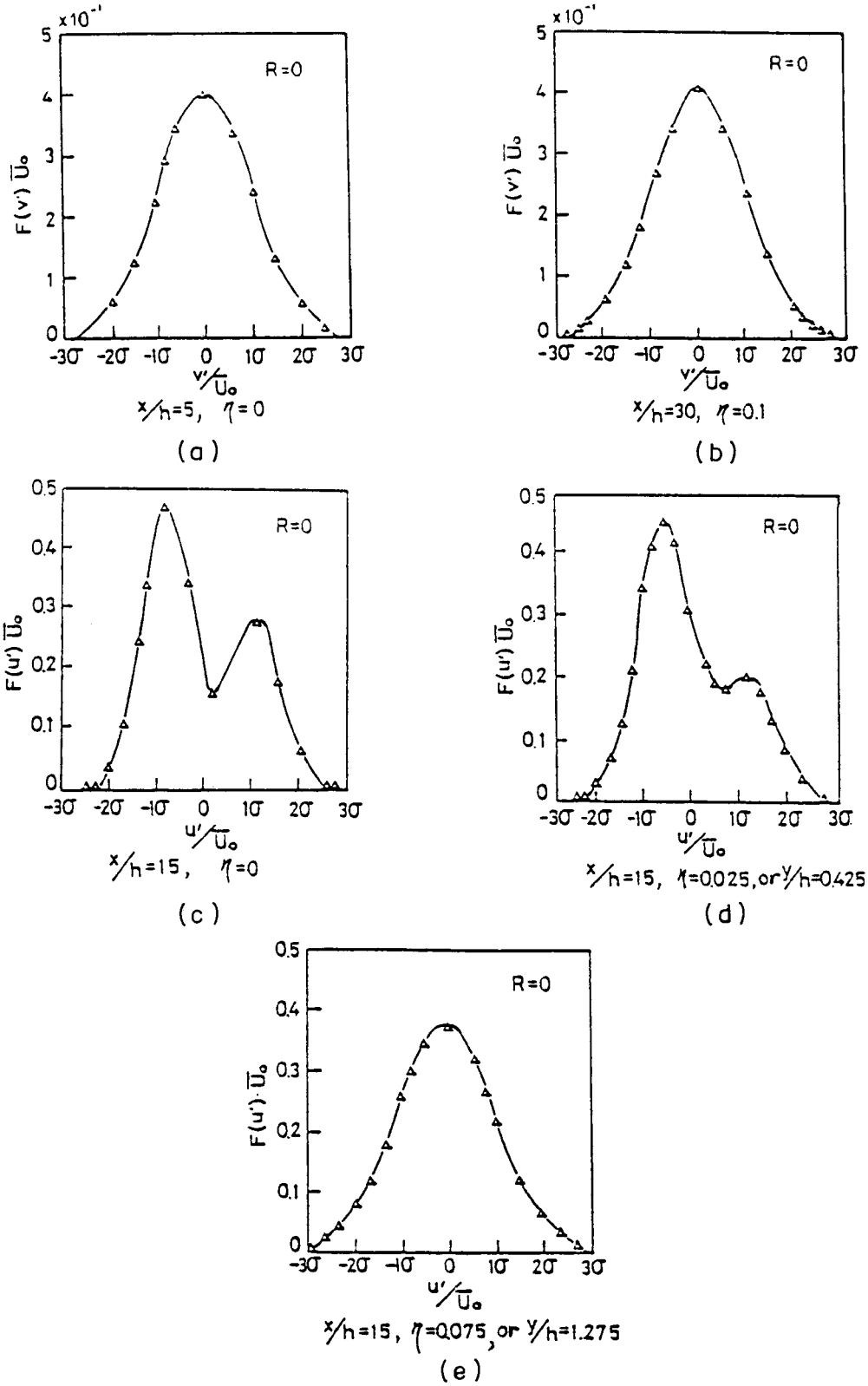

Figure 10. PDF ($R=0$)

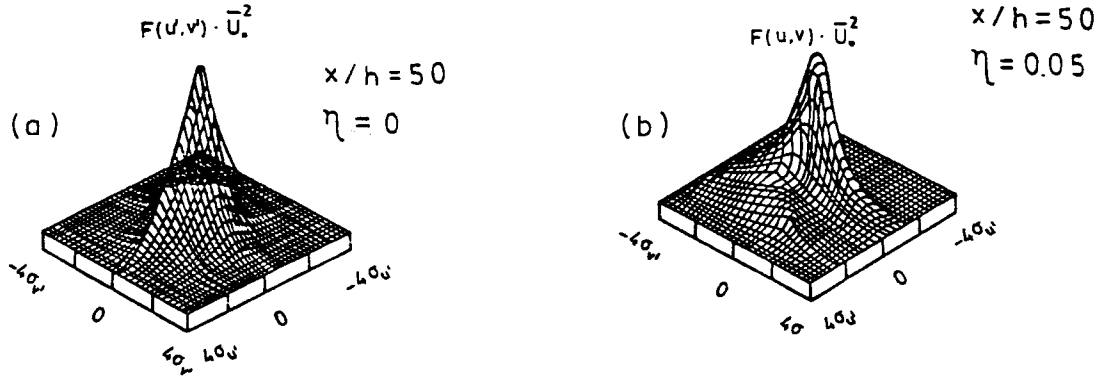

Figure 11. JPDF

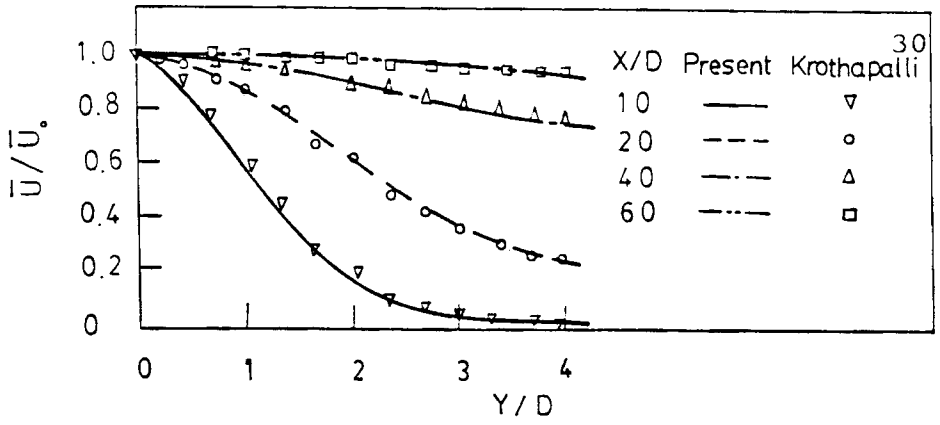

Figure 12. Mean velocity in x-direction ($n=5$)

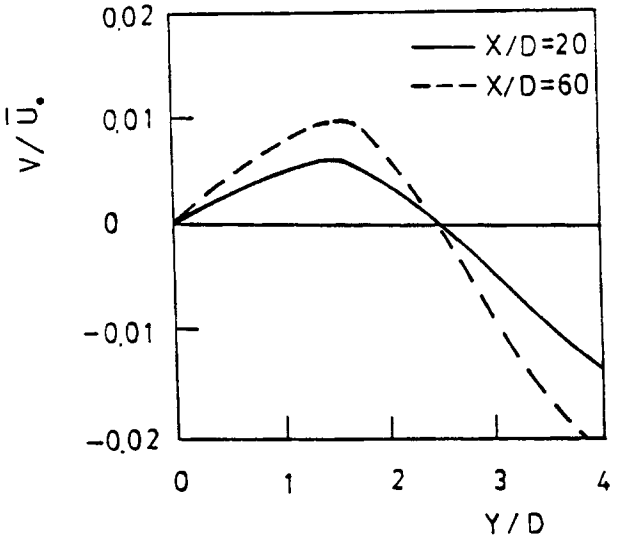

Figure 13. Mean velocity in y-direction ($n=5$)

Turbulence intensity. The turbulence intensity of the central jet along the centreline is shown in Figure 14. The calculated results are compared with Krothapalli's[30] data and show good agreement. The largest turbulence intensity is at $X/D=10$, because the maximum velocity difference is reached in this region.

Turbulence energy. The turbulence energy distributions in various regions are shown in Figure 15. Again the calculated results show good agreement with the experimental data of Krothapalli.[30] The correlations of the flow field for $X/D>60$ become weak and homogeneous, so the turbulence energy is smaller.

PDF. For the PDF the standard deviation is taken as the cross-co-ordinate unit, i.e.

$$\sigma_{u'}=(\bar{u}'^2)^{1/2}/\bar{U}_0, \qquad \sigma_{v'}\equiv(\bar{v}'^2)^{1/2}/\bar{U}_0, \qquad \sigma_{w'}=(\bar{w}'^2)^{1/2}/\bar{U}_0.$$

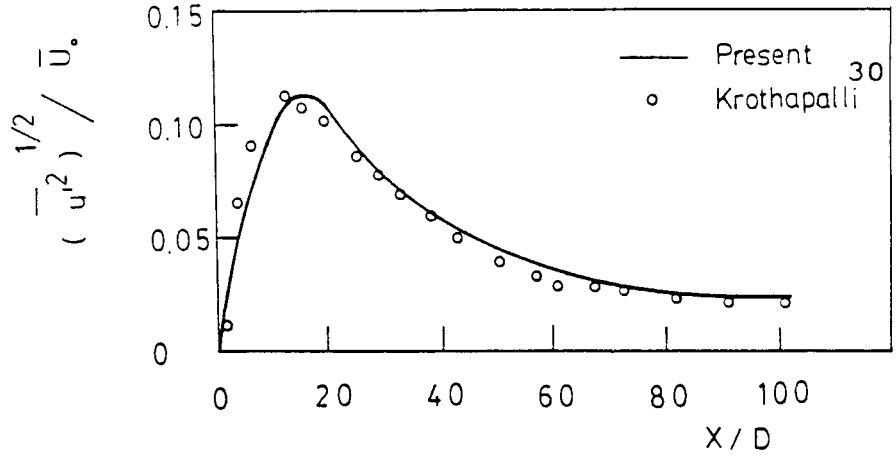

Figure 14. Turbulence intensity distribution along the axial axis ($n=5$)

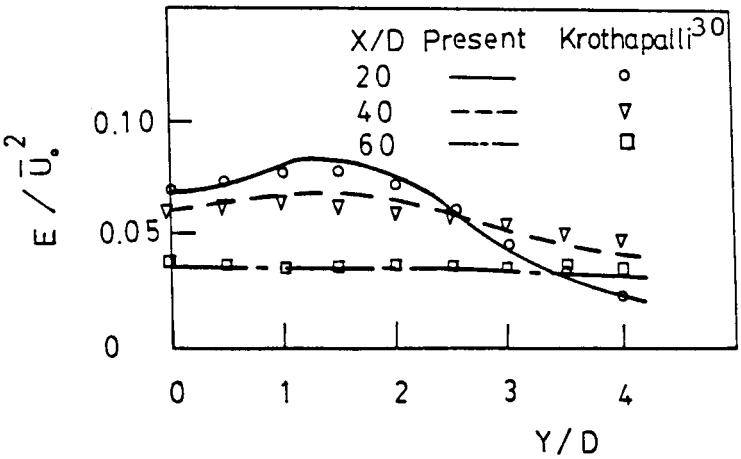

Figure 15. Turbulence energy distribution ($n=5$)

The distributions of $f(u')$ are shown in Figures 16(a)–16(c). The PDF at $X/D=20$, $Y/D=0$, shown in Figure 16(a), has two peaks, one arising from the negative u' from low-velocity eddies and the other arising from the positive u' from local eddies. The characteristics of this PDF distribution show that the local turbulence property results from the interaction between the two different eddy characteristics. The interaction between different eddies plays an important role in the mixing and growth of multiple jets. For the outer region at the same cross-section, the PDF distributions are shown in Figure 16(d) ($Y/D=2$) and Figure 16(g)($Y/D=4$). For $Y/D=2$ the PDF distribution deviates further from Gaussian because the turbulence correlations of the multiple jets at this location are strong. For $Y/D=4$ the PDF distribution approaches Gaussian because of the free stream region. The PDF distributions at $X/D=40$ are shown in Figures 16(b), 16(e) and 16(h). This is a B^2 region, so the correlations between momentum fluctuations are stronger than at $X/D=20$. The PDFs at $X/D=60$ are shown in Figures 16(c), 16(f) and 16(i). The distributions are close to Gaussian because the turbulent mixing is gradual decaying and the turbulence field is more homogeneous than in region B.

JPDF and turbulent transport. The distributions of the JPDF $F(u', v')$ at $X/D=20$ are shown in Figures 17(a)–17(d). For $Y/D=0$ the distribution is symmetrical with respect to the axis $\sigma_{v'}=0$ and the corresponding correlations of $\langle u'v' \rangle$ are zero, as shown in Figures 17(a) and 18. For

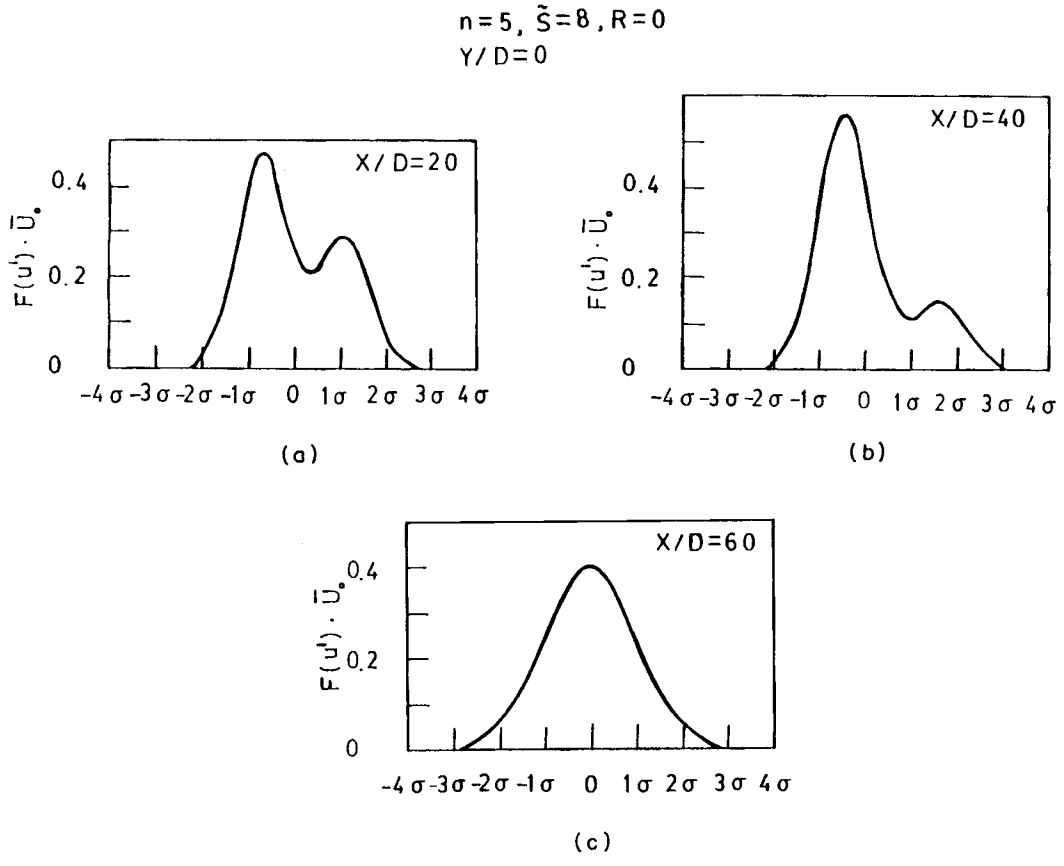

Figure 16. PDF ($n=5$)

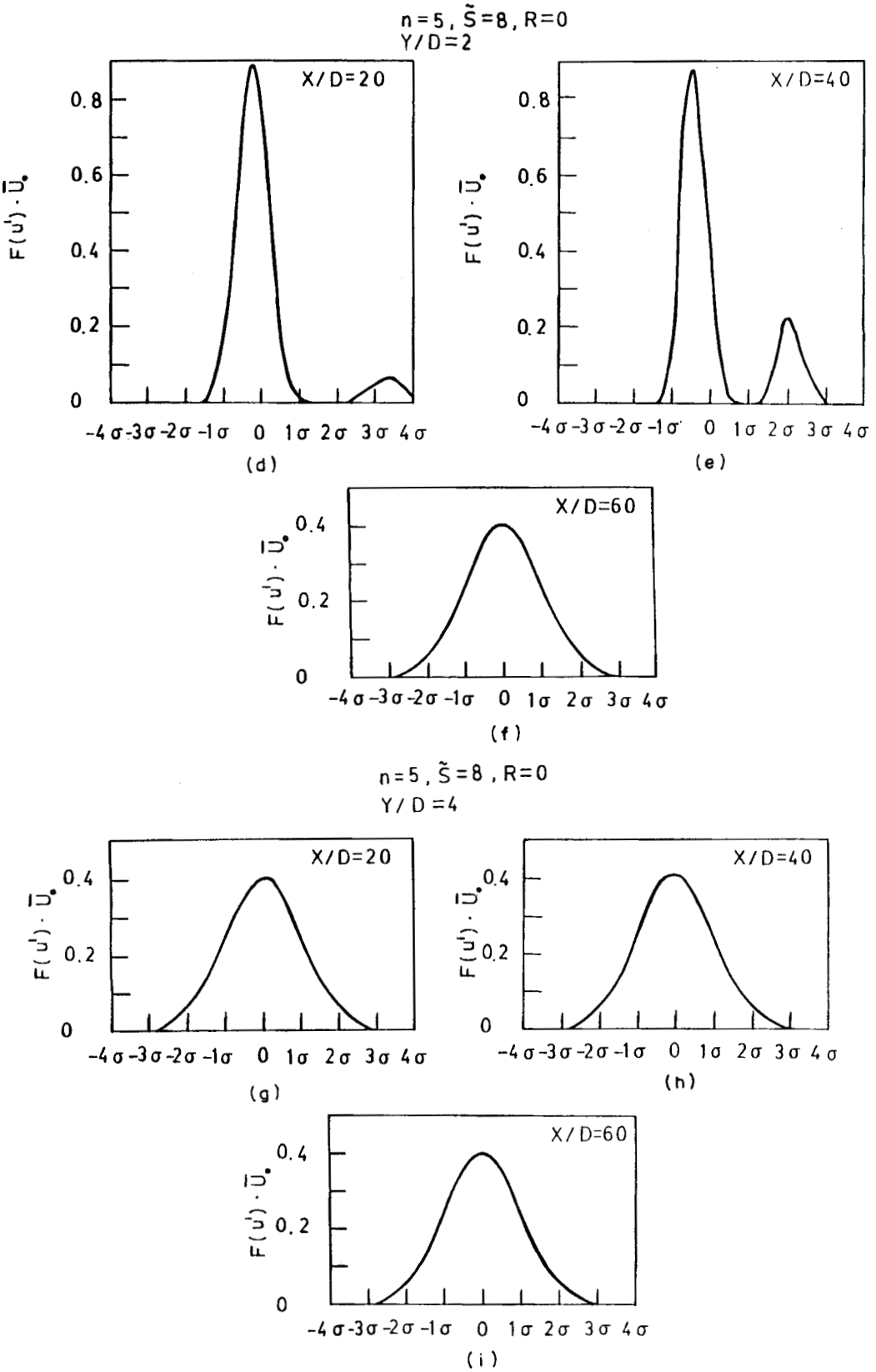

Figure 16 (Continued)

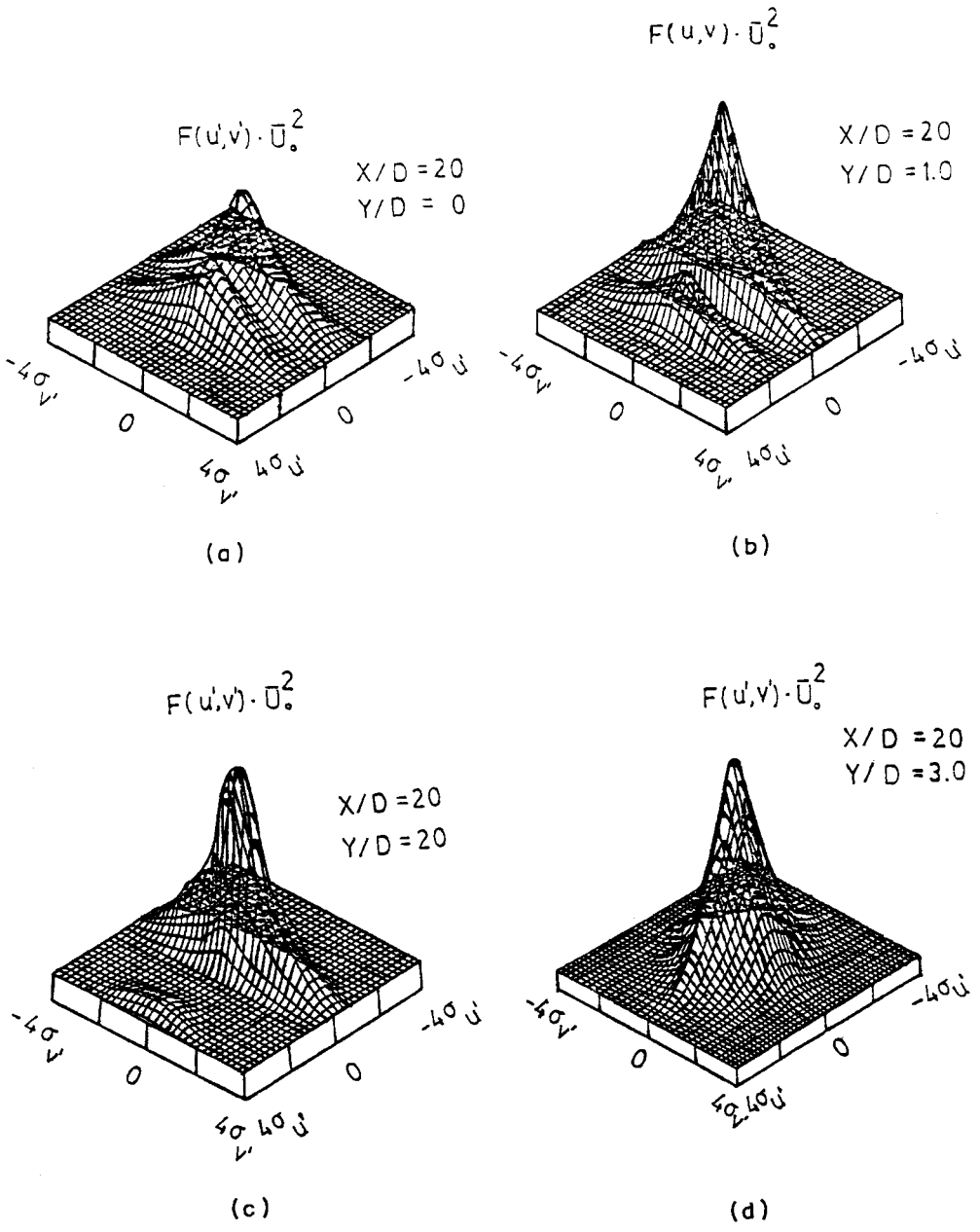

Figure 17. JPDF ($n=5$)

$Y/D=1$ and 2 the JPDFs deviate to the negative axes $\sigma_{u'}$ and $\sigma_{v'}$ and the correlations of $\langle u'v' \rangle$ are strong and positive, as shown in Figures 17(b), 17(c) and 18. For $Y/D=3$ the JPDF distribution approaches Gaussian, so the correlations of $\langle u'v' \rangle$ are small, as shown in Figures 17(d) and 18. The calculated results for the Reynolds stress at various sections are shown in Figure 18; they compare very well with Krothapalli's[30] data. One can clearly understand the internal structure of

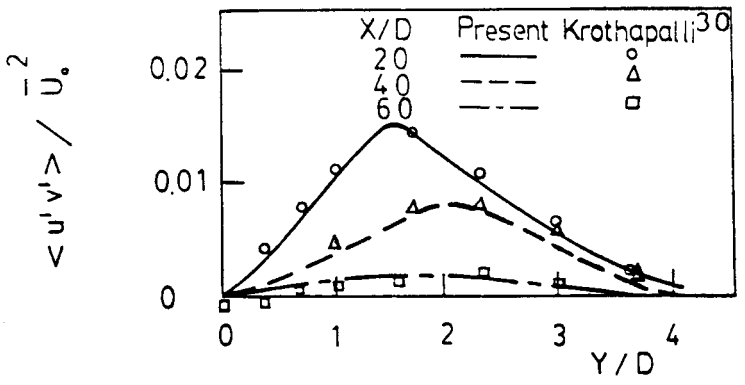

Figure 18. Reynolds stress distribution ($n=5$)

the Reynolds shear stress due to the corresponding distribution of the JPDF. Therefore the Reynolds shear stress structure of transport phenomena are better described in velocity space via the revealed JPDF in the transported direction.

One of the benefits of the kinetic theory of turbulence approach is that it can generate the various order correlations without using the conventional eddy viscosities. The third-order correlations of the turbulence energy transport terms, $\langle u'^2 v' \rangle$, are calculated as shown in Figure 19. The turbulence energy transport in the region between centreline and free stream is high because the eddy transport there is strong. At the centreline and in the free stream the turbulence energy transport is close to zero because of the distribution of $f(v')$ being close to Gaussian. The calculation of third-order moments via conventional turbulence modelling is very difficult and tedious. First one has to construct the moment equations for the third-order correlations and then try to close the fourth-order moments and many other fluctuation gradient correlations appearing in the equation. Numerous constants and transport coefficients will emerge and many will require experiments to justify those undetermined constants. The present

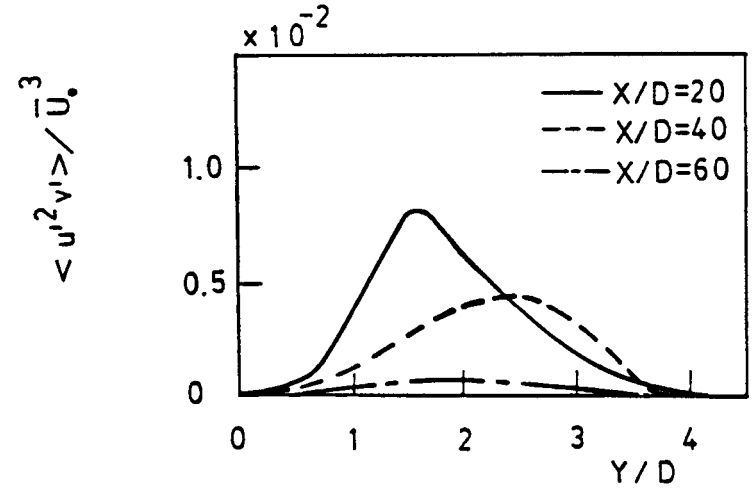

Figure 19. Turbulence energy transport ($n=5$)

kinetic theory of turbulence approach along with the modified Green's function method seems better justified in the sense of generating the moments, and the mixing mechanism seems to be better understood via the revealed PDFs and JPDFs.

Synthetic analysis of various multiple-plane-jet turbulent mixing

In order to utilize Krothapalli's[30] experimental data, we first analyse five-jet turbulent mixing. Then the individual jets are closed sequentially and we perform the turbulent mixing analysis for different numbers of jets ($n=1$–5). In order to compare the correlations among the various numbers of jets ($n=1$–5), the parameters are chosen as $X/D=30$, $S/D=8$ and $\bar{U}_\infty/\bar{U}_j=0$.

PDF. The distributions of $f(u')$ are shown in Figures 20(a)–20(h). For $Y/D=2$ the PDF of the single jet ($n=1$) approaches a Gaussian distribution because this region ($X/D=30$) is the fully developed flow for a single jet. For $Y/D=10$ the PDF distribution of twin jets is Gaussian because

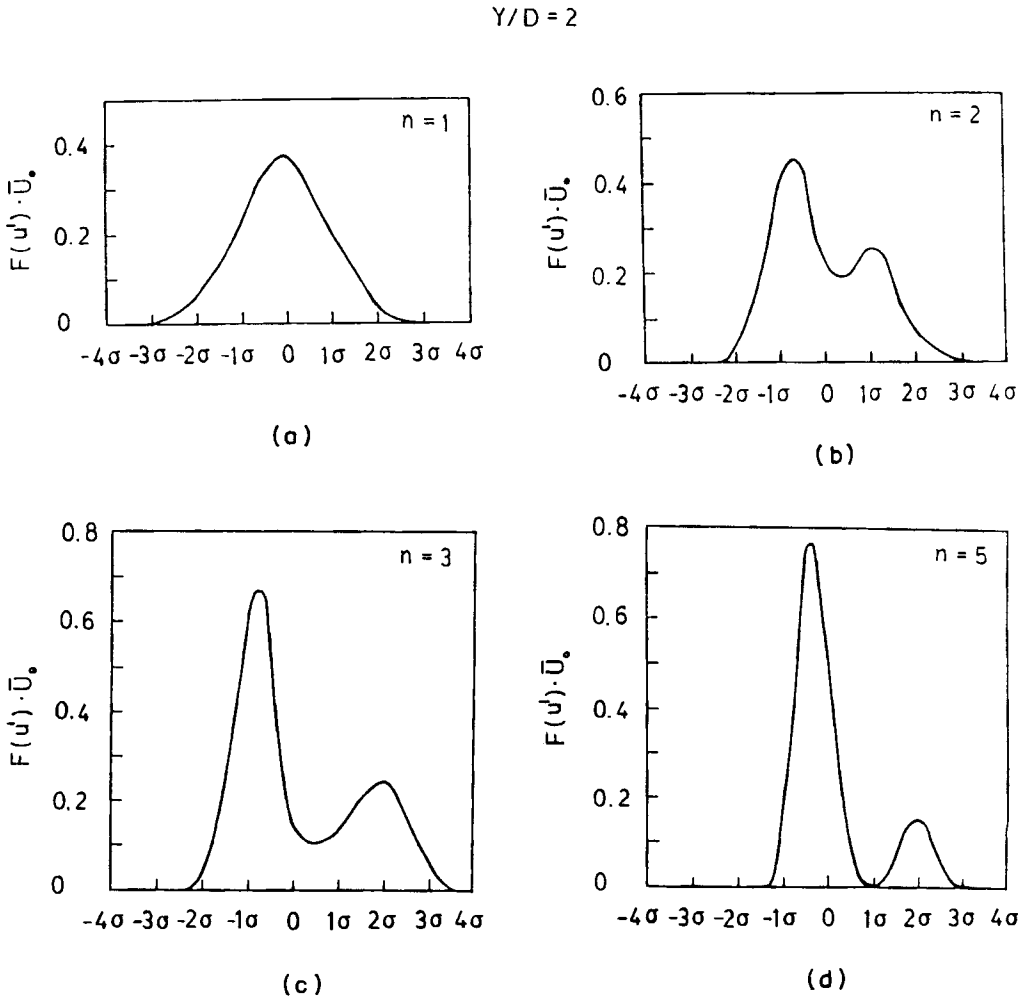

Figure 20. PDF ($n=5$)

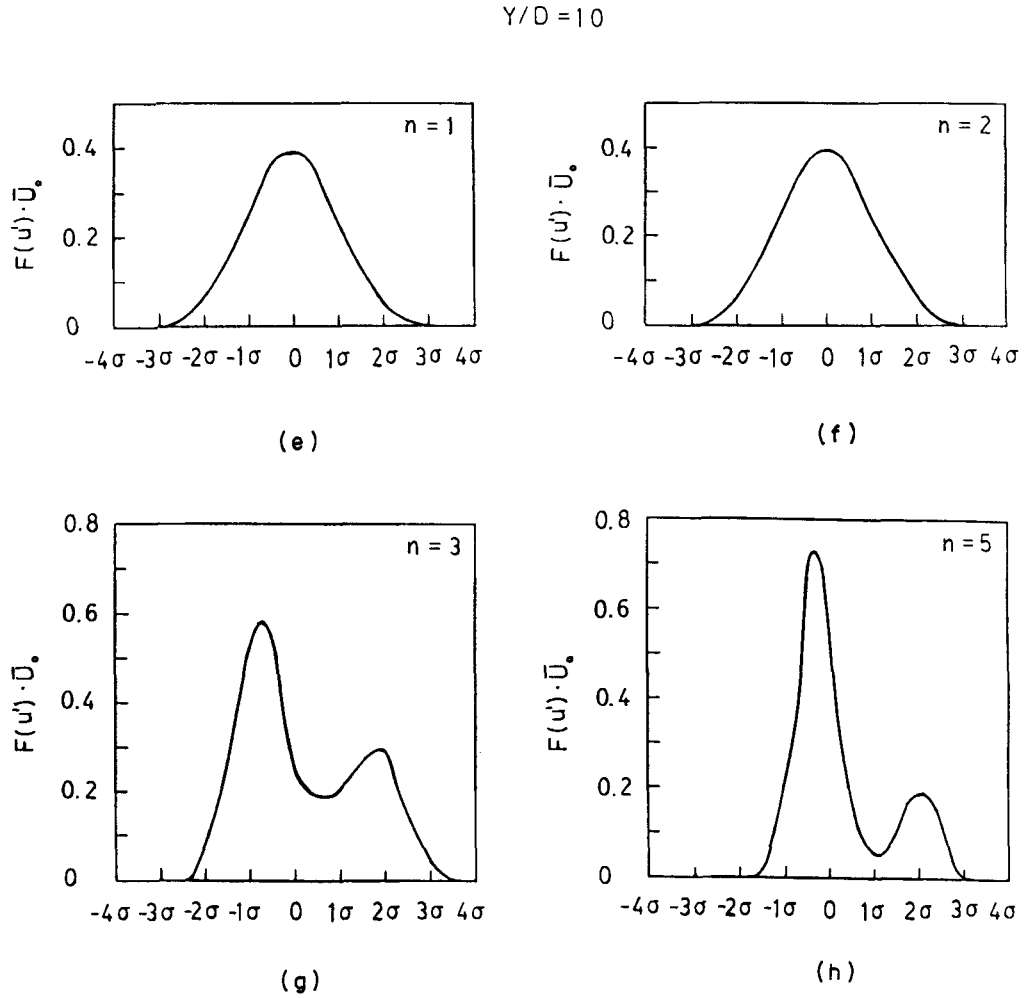

Figure 20 (Continued)

this location is the free stream for twin jets. The PDF distributions of multiple jets deviated from Gaussian because they are located in the interaction region among the various multiple jets.

Mean velocity. The mean velocities in the x-direction are shown in Figures 21(a)–21(d). From these calculated results the growth and decay phenomena of the momentum field among the various numbers of jets are better described via the revealed mutual interactions among the jets. This phenomenon can provide further understanding of the structure of multiple-jet mixing.

Turbulence energy. The turbulence energies are shown in Figure 22. The turbulence energies for $n=1$ and $n=2$ are similar. The turbulence energy distributions for $n=3$ and $n=5$ are wavy owing to the interaction of the second and third jets (symmetric to the axial axis).

Reynolds stress. The Reynolds stress distributions are shown in Figure 23. The distributions are wavy because the interactions among the multiple jets make the PDF distributions deviate from Gaussian.

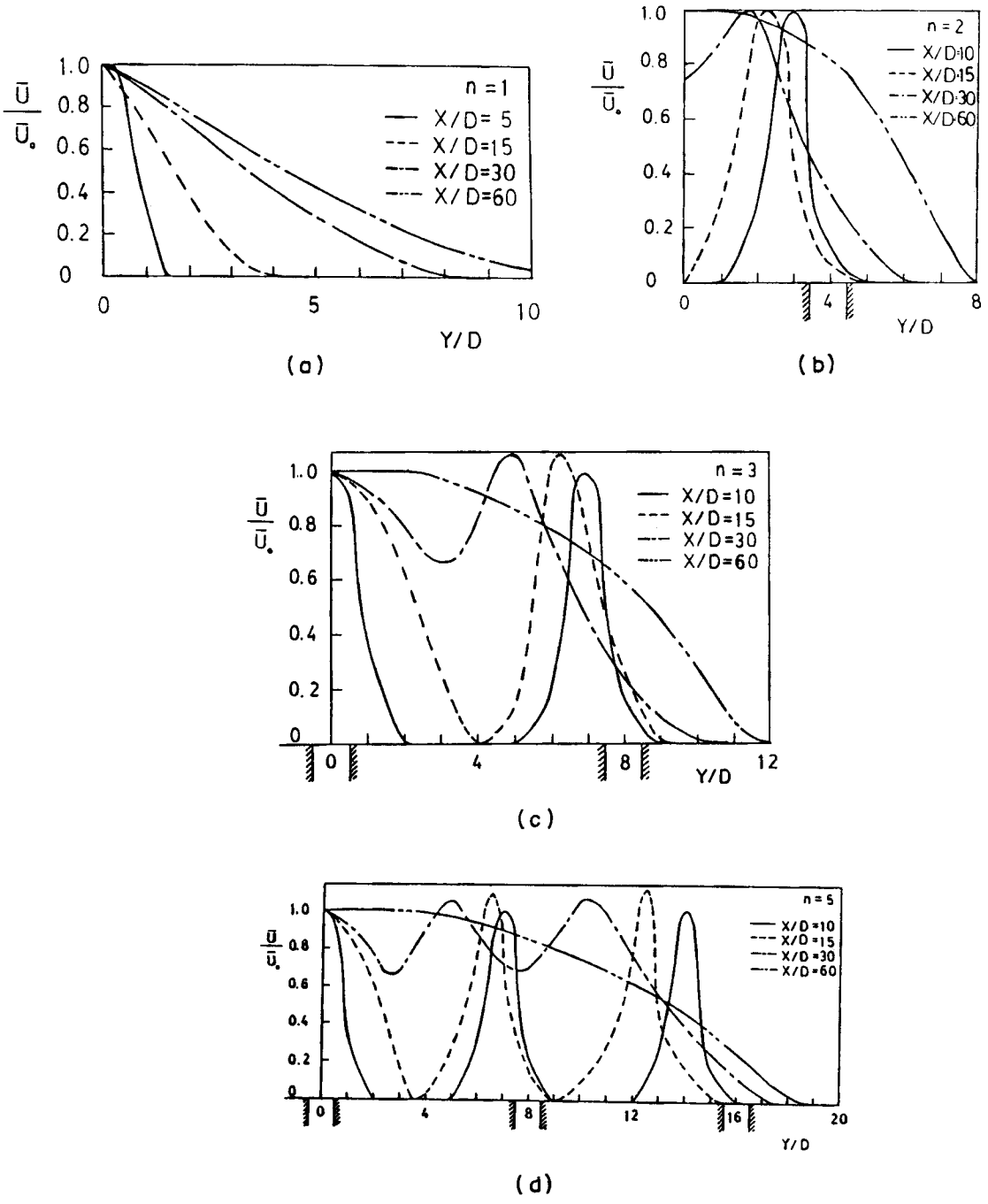

Figure 21. Mean velocity ($n = 1$–5)

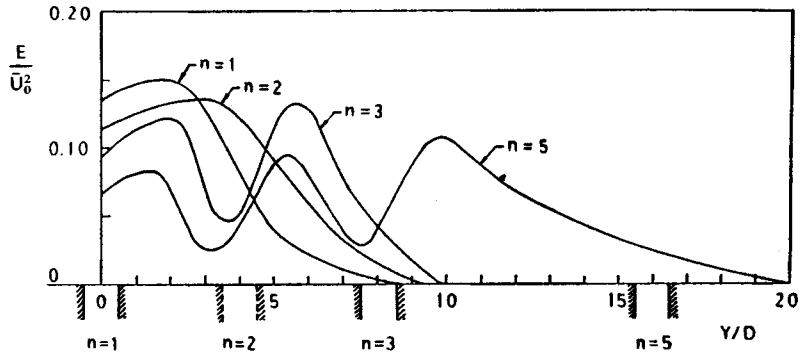

Figure 22. Turbulence energy as a function of n

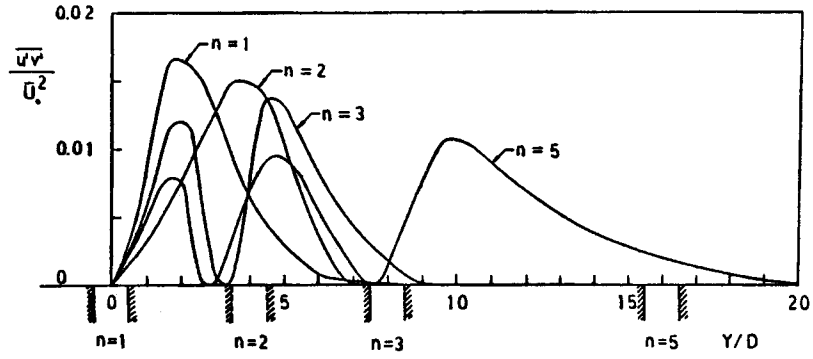

Figure 23. Reynolds stress as a function of n

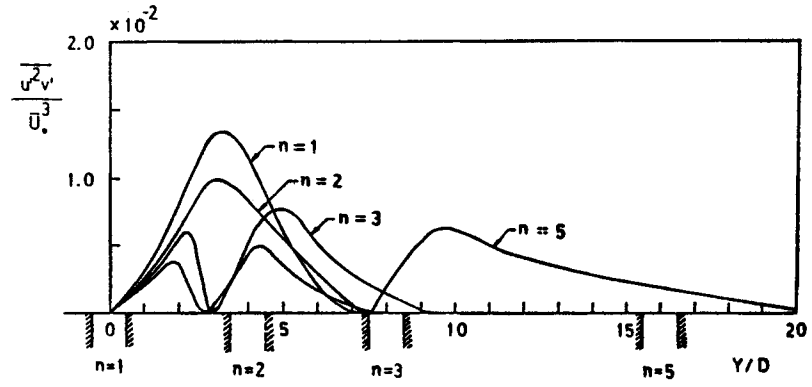

Figure 24. Turbulence energy transport as a function of n

Turbulence energy transport. The turbulence energy transports are shown in Figure 24. There are two and three peaks for $n=3$ and $n=5$ respectively because the local turbulence transport property resulted from interaction of three and five different eddy characteristics.

CONCLUSIONS

The real PDF of fluid elements in velocity space is revealed in the present analysis of multiple-jet turbulent mixing via a kinetic theory approach and the Green's function method. Since turbulent mixing has to be treated statistically, the real internal dynamic behaviour of the multiple-jet flow can be shown from the PDF of the fluid elements in velocity space. The mean flow quantities for the turbulent mixing of single, twin, triple and five jets have been synthetically analysed and the calculated results compare well with the available experimental data. For a single jet the turbulent jet in the initial region can be considered as two half-jets. This phenomenon signifies that the fluid element is affected by two different eddies from different streams, each still retaining its original characteristic (memory). For five jets the flow characteristics are divided into three regions: (1) the free jet region ($X/D<15$); (2) the transition region ($15\leqslant X/D\leqslant 60$); (3) the fully developed region ($X/D>60$). The mixing mechanism and Reynolds stress of the transition region are better described via the present corresponding revelaed JPDF. The higher-order correlations and turbulent transport phenomena of the mutual interaction of multiple jets can be easily predicted and explained (in contrast to the conventional phenomenological theory) in velocity space via the revealed PDF. Studies of multiple plane jets will provide some basic understanding of the mutual interaction of multiple jets and further application to the flame structure of gas burners, because the flame structure is affected by the mutual interaction of multiple jets.

APPENDIX: NOMENCLATURE

D	width of jets
E	turbulence energy $(\overline{u'^2}+\overline{v'^2}+\overline{w'^2})$
F	probability density function
f	PDF of fluid element
f_0	source condition of PDF
$f(u'), f(v'), f(w')$	PDFs of fluctuation velocities in x-, y- and z-directions respectively
$f(u', v')$	joint PDF of fluctuation velocities in x- and y-directions
G	Green's functions
h	width of single jet
MP	merge point
n	number of jets
S	space of jets
S_0	source condition at $x=0$
t	time
$\bar{U}_j$	velocity of jet at nozzle inlet
$\bar{U}_M$	velocity of mixing centre
$\bar{U}_0$	relative velocity $(\bar{U}_M-\bar{U}_\infty)$
$\bar{U}_\infty$	velocity of surroundings
u, v, w	instantaneous velocities in x-, y- and z-directions respectively
u', v', w'	fluctuation velocities in x-, y- and z-directions respectively
$\bar{U}, \bar{V}, \bar{W}$	mean velocities in x-, y- and z-directions respectively
X	co-ordinate of jet axis
Y	co-ordinate of y-axis
β_1	characteristic relaxation rate of energy-containing eddies
β^v	characteristics relaxation rate of microscale

ω	chemical reaction term
Λ_1	characteristic scale of energy-containing eddies

Subscripts and superscripts

$\langle\ \rangle$	ensemble average vector
∞	free stream condition
0	source condition
i	jet number
j	tensor

REFERENCES

1. J. H. Wang, 'Plane jet turbulent mixing and combustion' (in Chinese), *Master Thesis*, Department of Mechanical Engineering, National Taiwan University, 1978.
2. Z. C. Hong and S. H. Chuang, 'Kinetic theory approach to twin plane jets turbulent mixing analysis', *AIAA J.*, **26,** 303–310 (1988).
3. T. S. Lundgren, 'Distribution functions in the statistical theory of turbulence', *Phys. Fluids*, **10,** 969–975 (1967).
4. T. S. Lundgren, 'Model equation for non-homogeneous turbulence', *Phys. Fluids*, **12,** 485–497 (1969).
5. R. J. Fox, 'Solution for the correlation functions in a homogeneous isotropic incompressible turbulent field', *Phys. Fluids*, **14,** 1806–1808 (1971).
6. R. J. Fox, 'Distribution functions in the statistical theory of compressible turbulent fluids', *Sandia Laboratories Report SAND 74-0119*, 1974.
7. J. T. Yen, 'Kinetic theory of turbulent flow', *Phys. Fluids*, **15,** 1728–1734 (1972).
8. D. C. Haworth and S. B. Pope, 'A generalized Langevin model for turbulent flows', *Phys. Fluids*, **29,** 387–405 (1986).
9. D. C. Haworth and S. B. Pope, 'A pdf modeling study of self-similar turbulent free shear flows', *Phys. Fluids*, **30,** 1026–1044 (1987).
10. S. B. Pope, 'Consistency conditions for random-walk models of turbulent dispersion', *Phys. Fluids*, **30,** 2374–2379 (1987).
11. S. B. Pope, 'Consistent modeling of scalars in turbulent flows', *Phys. Fluids*, **26,** 404–408 (1983).
12. H. van Dop, F. T. M. Nieuwstadt and J. C. R. Hunt, 'Random walk models for particle displacements in inhomogeneous unsteady turbulent flows', *Phys. Fluids*, **28,** 1639–1653 (1985).
13. B. L. Sawford, 'Generalized random forcing in random-walk turbulent dispersion models', *Phys. Fluids*, **29,** 3582–3585 (1986).
14. P. M. Chung, 'Turbulent chemically reacting flows', *Aerospace Corporation Technical Report TR-1001 (S2855-20)-5*, 1967.
15. P. M. Chung, 'A simplified statistical model of turbulent chemically reacting shear flows', *AIAA J.*, **7,** 1982–1991 (1969).
16. P. M. Chung, 'Chemical reaction in a turbulent flow field with uniform velocity gradient', *Phys. Fluids*, **13,** 1153–1165 (1970).
17. P. M. Chung, 'On the development of diffusion flame in homologous turbulent shear flows', *AIAA Paper 70-722*, 1970.
18. P. M. Chung, 'Diffusion flame in homologous turbulent shear flows', *Phys. Fluids*, **15,** 1735–1746 (1972).
19. P. M. Chung, 'Turbulent diffusion flame in Couette flow', *AIAA Paper 72 214*, 1972.
20. P. M. Chung and H. T. Shu, 'HF chemical laser amplification properties of a uniform turbulent mixing layer', *Acta Astronaut.*, **1,** 835 (1974).
21. P. M. Chung, 'A kinetic-theory approach to turbulent chemically reacting flows', *Comb. Sci. Technol.*, **13,** 123–153 (1976).
22. Z. C. Hong, 'Turbulent chemically reacting flows according to a kinetic theory', *Ph.D. Dissertation*, Department of Energy Engineering, University of Illinois at Chicago, 1975.
23. Z. C. Hong and Z. C. Lai, 'On the mixing analysis of a free turbulence shear layer', *Proc. 1st Conf. on Theoretical and Applied Mechanics*, R.O.C., 1977, pp. 173–192.
24. S. Corrisin, 'Investigation of the behavior of parallel two-dimensional air jets', *NACA W-90*, 1944.
25. C. J. Laurence and N. J. Benninghoff, 'Turbulent measurements in multiple interfering air jets', *NASA TN4029*, 1957.
26. F. G. Marsters, 'Measurements in the flow field of a linear array of rectangular nozzles', *AIAA Paper 79-0350*, 1979.
27. R. Knystautas, 'The turbulent jet from a series of holes in line', *Aeronaut. Q.*, **XV,** 1–28 (1964).
28. N. T. Aiken, 'Aerodynamic and noise measurements on a quasi-two dimensional augmenter wing model with lobe-type nozzles', *NASA TMX-62*, 237, 1973.
29. A. Krothapalli, 'An experimental study of multiple jet mixing', *Ph.D. Dissertation*, Standford University, 1979.
30. A. Krothapalli, 'Development and structure of a rectangular jet in a multiple jet configuration', *AIAA J.*, **18,** 945–950 (1980).

31. R. J. Bywater, 'Velocity space description of certain turbulent free shear flow characteristics', *AIAA J.*, **19,** 969–975 (1981).
32. R. J. Bywater, 'Numerical solutions of a reduced pdf model for turbulent diffusion flames', *AIAA J.*, **20,** 824–830 (1982).
33. B. W. Spencer, 'Statistical investigation of turbulent velocity and pressure fields in a two-stream mixing layer', *Ph.D. Dissertation*, University of Illinois, 1970.
34. S. C. Lee and P. T. Harsha, 'Use of turbulent kinetic energy in free mixing studies', *AIAA J.*, **18,** 1026–1038 (1970).
35. S. H. Chuang, 'Kinetic theory approach of the multiple plane jets turbulent mixing, combustion and HF chemical laser analysis' (in Chinese), *Ph.D. Dissertation*, National Taiwan University, 1986.
36. G. K. Batchelor, *The Theory of Homogeneous Turbulence*, Cambridge University Press, Cambridge, 1960.
37. E. Gutmark and I. Wygnanski, 'The planar turbulent jet', *J. Fluid Mech.*, **73,** 456–495 (1976).
38. L. J. S. Bradbury, 'The structure of a self-preserving turbulent plane jet', *J. Fluid Mech.*, **23,** 31–64 (1965).
39. Z. C. Hong and S. H. Chuang, 'Kinetic theory approach of the five plane jets turbulent mixing analysis', *J. CSME*, **7,** 361–372 (1986).